Atomic and molecular hydrogen elimination in the crossed beam reaction of d1-ethinyl radicals C$_2$D(X $^2\Sigma^+$) with acetylene, C$_2$H$_2$(X $^1\Sigma_g^+$): Dynamics of d1-diacetylene (HCCCCD) and d1-butadiynyl (DCCCC) formation†

R. I. Kaiser,*[a] **F. Stahl,**[bc] **P. v. R. Schleyer**[bc] **and H. F. Schaefer III**[c]

[a] *Department of Chemistry, University of York, York, UK YO10 5DD. E-mail: rik1@york.ac.uk*
[b] *Institut für Organische Chemie der Universität Erlangen-Nürnberg, 91054, Erlangen, Germany*
[c] *Center for Computational Quantum Chemistry, The University of Georgia, Athens, GA 30602, USA. E-mail: schleyer@chem.uga.edu*

The chemical reaction dynamics to form d1-diacetylene, DCCCCH (X $^1\Sigma^+$), and the d1-butadiynyl radical, DCCCC, *via* the reaction of d1-ethinyl, C$_2$D (X $^2\Sigma^+$), with acetylene, C$_2$H$_2$ (X $^1\Sigma_g^+$), are explored in a crossed molecular beam experiment at an average collision energy of 26.1 kJ mol^{-1}. The experiments show that the reaction follows indirect scattering dynamics *via* a C$_4$H$_2$D intermediate. The calculations confirm that the reaction has no entrance barrier and that it proceeds *via* an attack of the ethinyl radical on the π electron density of the acetylene molecule. The initially formed *trans*-1-d-ethinylvinyl-2 (HCCHC$_2$D) intermediate rearranges to its *cis* form; the latter is found to fragment predominantly *via* H atom emission to form d1-diacetylene, HCCCCD (X $^1\Sigma^+$) and H (^{2}S$_{1/2}$) (channel 1). A second involves a [1,2]-H shift in *trans*-HCCHC$_2$D to yield a 1-d-ethinylvinyl-1 radical. The latter channel then shows two fragmentation pathways: a molecular hydrogen elimination to form the d1-butadiynyl radical (DCCCC) (channel 2) and an atomic hydrogen loss to yield d1-diacetylene (HCCCCD) (channel 3). Compared to the C$_4$HD/H products (98–99%), the C$_4$D/H$_2$ channel presents only a minor pathway (1–2%). The solid identification of diacetylene under single collision conditions is the first experimental proof of a long-standing hypothesis that the title reaction can synthesize diacetylene in dark, molecular clouds, the outflow of dying carbon stars, hot molecular cores, as well as in the atmospheres of hydrocarbon rich planets and satellites such as the Saturnian moon Titan.

I. Introduction

The diacetylene molecule (HCCCCH, X $^1\Sigma_g^+$) is ubiquitous in the interstellar medium (ISM)[1] and in the hydrocarbon rich planetary atmospheres of Saturn and its moon Titan. In planetary environments, diacetylene serves as an ultraviolet radiation shield.[2] In analogy to ozone protecting Earth from ultraviolet photons, diacetylene absorbs these destructive ultraviolet photons to preserve the lower atmospheric layers and surfaces of planets and their moons. Photochemical models of Jupiter, Saturn, Uranus, Neptune, Pluto and their satellites Titan and Triton also predict that diacetylene is the key intermediate in the synthesis of more complex polyynes such as triacetylene (HCCCCCCH), tetraacetylene (HCCCCCCCCH), and possibly even the visible haze layers.[3]

Despite this fundamental role in atmospheric chemistry, the formation mechanism of diacetylene remains speculative: diacetylene is postulated to result uniquely from the reaction of the ethinyl radical (C$_2$H, X $^2\Sigma^+$) with acetylene (C$_2$H$_2$, X $^1\Sigma_g^+$) as the sole reaction product.[4] Though this hypothesis still lacks experimental verification, it manifests the basis for photochemical models which are in poor quantitative agreement with results from Voyager I/II observations.[5] Hence, accurate experimental data are of particular importance to modelers of planetary chemistry. Furthermore, the Cassini–Huygens mission to Titan is scheduled to arrive in the Saturnian system in 2004.[6] For a meaningful interpretation of the vast amount of new atmospheric data that will be recorded, an understanding of the most fundamental processes such as the formation of diacetylene and the role of the reaction of ethinyl radicals with acetylene is truly essential.

Recent laboratory kinetics studies on this system at temperatures from 295 K to 15 K demonstrated that the reaction of ethinyl radicals with acetylene proceeds very rapidly ($k = 0.94 - 2.7 \times 10^{-10}$ cm^3 s^{-1}),[7] which suggests no or only a minor entrance barrier for this process. The missing information from these kinetic studies is the nature of the intermediates involved and, in particular, the nature of the reaction products. This lack of detail hampers a refinement of the photochemical models and calls for a scrutiny of this important reaction at the most fundamental, microscopic level. Here, we report on a crossed molecular beam investigation augmented by electronic structure calculations on the partially deuterated variant of the ethinyl radical plus acetylene reaction (1)–(3), *i.e.* d1-ethinyl radicals (C$_2$D) with acetylene (C$_2$H$_2$).[8] This system represents *the* prototype reaction of ubiquitous ethinyl radicals with the simplest, closed shell unsaturated hydrocarbon, acetylene, to form diacetylene and/or its isomer(s) and potentially butadiynyl radicals in hydrocarbon rich atmospheres of planets and their moons *via* a single collision event.[9] In Saturn's moon, Titan, for example, short wavelength photons ($\lambda < 200$ nm) can penetrate to the stratosphere and dissociate acetylene to atomic hydrogen plus an ethinyl

radical.[10] The reaction of the ethinyl fragment with undissociated acetylene to form complex C_4 hydrocarbons is expected.

$$C_2D \ (X \ ^2\Sigma^+) + C_2H_2 \ (X \ ^1\Sigma_g^+) \rightarrow DCCCCH \ (X \ ^1\Sigma^+)$$
$$+ \ H \ (^2S_{1/2}), \quad (1)$$

$$\rightarrow H_2CCCC \ (X \ ^1A_1) + D \ (^2S_{1/2}), \quad (2)$$

$$\rightarrow DCCCC \ (X \ ^2\Sigma^+/A \ ^2\Pi) + H_2 \ (X \ ^1\Sigma_g^+). \quad (3)$$
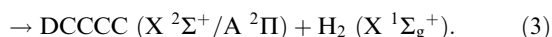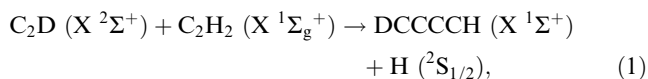
II.   Experiment and data processing

The experiments are carried out under single collision conditions coupling our d1-ethinyl, C_2D ($X \ ^2\Sigma^+$), source with the universal 35″ crossed molecular beam machine.[11] A pulsed supersonic ethinyl radical beam, C_2D ($X \ ^2\Sigma^+$), is generated *in situ via* laser ablation of graphite at 266 nm[12,13] and seeding the ablated species in neat deuterium which acts as a reactant gas as well. This source design leads to a number density of 0.5×10^{11} radicals cm^{-3} in the interaction region of the scattering chamber.[14] This beam contains further atomic carbon (C (^3P_j)), dicarbon (C_2 ($X \ ^1\Sigma_g^+$)), and (C_3 ($X \ ^1\Sigma_g^+$)). However, these species do not interfere with the reactive scattering signal of the C_2D/C_2H_2 system at $m/z = 51$ and 50 (IV.A): the C (^3P_j) + C_2H_2 ($X \ ^1\Sigma_g^+$) reaction leads to a reactive scattering signal at $m/z = 37$ (C_3H^+) and $36(C_3^+)$;[15] the C_2 ($X \ ^1\Sigma_g^+$)/ C_2H_2 ($X \ ^1\Sigma_g^+$) system gives rise to counts at mass to charge ratios not exceeding $m/z = 49$ (C_4H^+);[16] the reaction of C_3 ($X \ ^1\Sigma_g^+$) with C_2H_2 ($X \ \Sigma_g^+$) is endoergic by about 86 kJ mol^{-1} and hence closed under the present experimental conditions.[16] The pulsed d1-ethinyl beam passes the skimmer, and a four-slot chopper wheel mounted after the ablation zone selects a 9.0 μs segment of the pulse with a peak velocity v_p of $1790 + 30$ ms^{-1} and speed ratio S of 7.6 ± 0.2. This beam crosses an acetylene beam in the main chamber at a collision energy of 26.1 kJ mol^{-1} ($v_p = 900 \pm 10$ m s^{-1}, $S = 9.0$). The reactively scattered species are probed using a triply differentially pumped detector consisting of a Brink-type electron-impact-ionizer, quadrupole mass-filter, and a Daly ion detector[17] recording time-of-flight spectra (TOF) at different laboratory angles at mass to charge ratios $m/z = 51$ (C_4HD^+) and 50 ($C_4H_2^+$, C_4D^+) under ultrahigh vacuum conditions ($< 8 \times 10^{-13}$ torr). Integrating these TOFs at each laboratory angle and correcting for different data accumulation times yields the laboratory angular distribution (LAB). Data collection times are up to 30 h per angle. Information on the chemical reaction dynamics was gained by fitting the TOF spectra and the product angular distribution in the laboratory frame (LAB) using a forward-convolution routine.[18] This procedure initially assumes an angular distribution $T(\theta)$ and a translational energy distribution $P(E_T)$ in the center-of-mass reference frame (CM). Laboratory TOF spectra and (the laboratory) angular distributions were then calculated from $T(\theta)$ and $P(E_T)$. Best TOF and laboratory angular distributions were achieved by refining adjustable $T(\theta)$ and $P(E_T)$ parameters. The final outcome is the generation of a product flux contour map which reports the differential cross section, $I(\theta,u) \sim P(u) \ T(\theta)$, as the intensity as a function of angle θ and product velocity u in the center-of-mass reference frame. This plot contains all the information on the reactive scattering process.[18]

III.   Electronic structure calculations

All structures were optimized and confirmed as minima or transition states by frequency analysis at the UB3LYP/6-311+G** level of theory as implemented in Gaussian 98.[19]

The structures of the intermediate 1-ethinylvinyl-1 radical were also optimized at complete active space SCF (CASSCF)/6-311G* using the GAMESS suite of programs.[20] The chosen active space included the complete set of π-orbitals and the σ-orbital in which the unpaired electron might be located, *i.e.* CASSCF(7,7)/6-311G*. Single point energies for the reactants and products were also computed at CCSD(T)/cc-pVTZ with the ACES2 program[21] and the energies were corrected with unscaled B3LYP/6-311+G** ZPVEs. Furthermore, the G2 method[22] was applied to achieve chemical accuracy (± 5 kJ mol^{-1}) for the reaction enthalpies.

IV.   Results

A.   Reactive scattering signal and laboratory angular distributions (LAB)

Reactive scattering signal was recorded at mass-to-charge ratios $m/z = 51$ (C_4HD^+) and 50 ($C_4H_2^+$/C_4D^+); due to the presence of dicarbon in the primary beam, data at $m/z = 49$ and 48 were not recorded. No signal for the radiative association channel to C_4H_2D was found. At each laboratory angle, the TOF spectra of both mass to charge ratios differed and could not be superimposed. This finding alone demonstrates that at least two distinct products of the gross formula C_4HD ($m/z = 51$) and C_4H_2/C_4D ($m/z = 50$) are formed in the reaction of a d1-ethinyl radical with acetylene (single collision event, hence, only one C_2D). The signal at $m/z = 51$ can be attributed to a C_2D *versus* H exchange pathway; TOF spectra at $m/z = 50$ depict two components: (i) the C_4D^+ ions arising from cracking of the C_4HD^+ parent in the electron impact ionizer and (ii) a second channel which demonstrates the formation of C_4H_2 (C_2D *versus* D exchange) and/or C_4D isomers (C_2D *versus* H_2 exchange).

The important laboratory angular distribution (LAB) of the C_2D ($X \ ^2\Sigma^+$) + C_2H_2 ($X \ ^1\Sigma_g^+$) reaction at $m/z = 50$ is shown in Fig. 1 together with the calculated curves using the center-of-mass best fit functions at a collision energy of 26.1 kJ mol^{-1}. . The signal at $m/z = 51$ was fit with only one channel corresponding to the C_4HD product. However, applying this center-of-mass function to fit also the data at $m/z = 50$ clearly indicates that a second channel accounting for the fast part of the TOF spectra is missing (Fig. 2). The LAB distributions of both channels peaks at 27.0° close to the center-of-mass
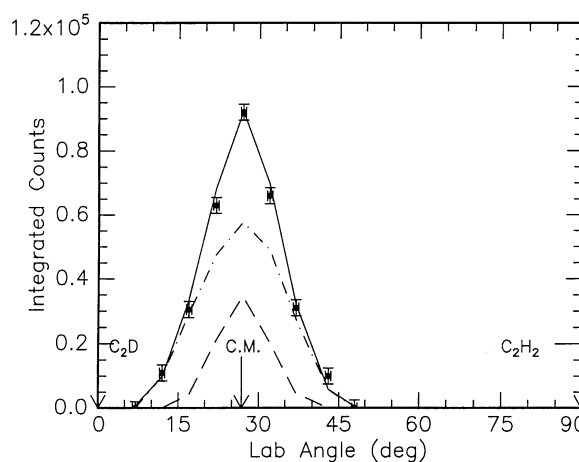
Fig. 1 Laboratory angular distribution of $m/z = 50$ for the $C_2D(X \ ^2\Sigma^+)$ + $C_2H_2(X \ ^1\Sigma_g^+)$ reaction. Circles and 1σ error bars indicate experimental data, the dashed lines the calculated distribution for d1-diacetylene product (DCCCCH; channel 1), the dashed-dotted line the calculated distribution for the d1-butadiynyl product (DCCCC; channel 2), and the solid line the sum. C.M. designates the center-of-mass angle.
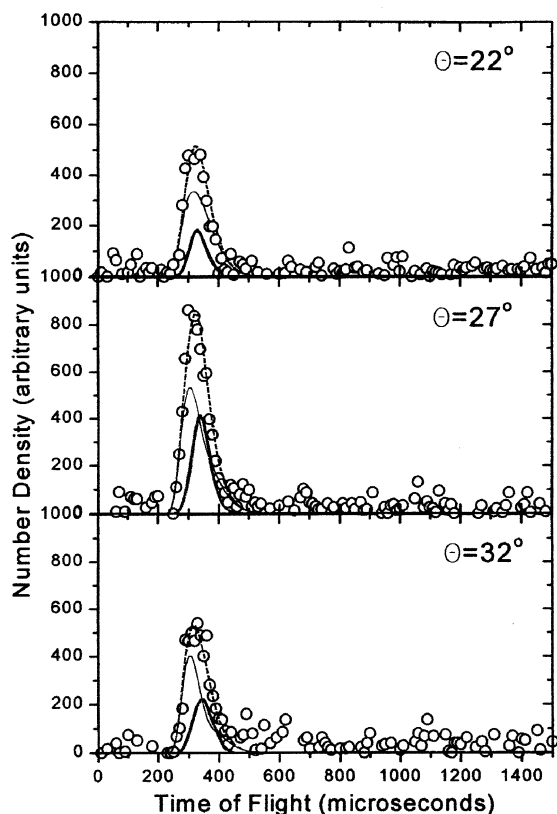
Fig. 2 Time-of-flight data of the $C_2D(X\ ^2\Sigma^+) + C_2H_2(X\ ^1\Sigma_g^+)$ reaction of $m/z = 50$ at three laboratory angles. The circles indicates the experimental data, the thin lines the calculated distribution for d1-diacetylene product (DCCCCH; channel 1), the thick lines the calculated distribution for the d1-butadiynyl product (DCCCC; channel 2), and the dashed lines the sum.

angle of $26.7 \pm 0.6°$, and the reactive scattering products are spread within 25° (fragmentation from $m/z = 51$) and 35° in the plane defined by both beams.

B. Center-of-mass flux contour maps, $I(\theta,u)$

Best fits of data at $m/z = 51$ were obtained with a single center-of-mass translational energy and angular distribution corresponding to the reaction $C_2D\ (X\ ^2\Sigma^+) + C_2H_2\ (X\ ^1\Sigma_g^+) \rightarrow C_4HD + H\ (^2S_{1/2})$. Data at $m/z = 50$ required a fit with two reaction channels, *i.e.* fragmentation of the C_4HD product and a second pathway $C_2D\ (X\ ^2\Sigma^+) + C_2H_2\ (X\ ^1\Sigma_g^+) \rightarrow C_4D + H_2\ (X\ ^1\Sigma_g^+)$. The underlying flux contour plots are shown in Fig. 3. Inspection of the center-of-mass velocity u of the products provides further insight into the energetics of both reaction channels. All the information included in u translates into information on the translational energy of the products and, hence, the center-of-mass translational energy distribution $P(E_T)$. The maximum translational energy E_{max} can be used to identify the nature of the products. E_{max} is simply the sum of the reaction exothermicity obtained either from electronic structure calculations or by comparison with literature data and the collision energy in our experiments. Therefore, reaction channel 1 with an experimentally determined E_{max}: 136–146 kJ mol^{-1} and a collision energy of 26 kJ mol^{-1}, is exothermic by 110–120 kJ mol^{-1}. The situation of the molecular hydrogen loss (channel 2) is more complicated. Within our experimental error limits (E_{max}: 20–30 kJ mol^{-1}), we cannot determine if the reaction is thermoneutral, slightly exothermic (−6 kJ mol^{-1}), or endothermic (+4 kJ mol^{-1}). Information about the energy of the exit transition state can be deduced from the distribution maximum of the relative
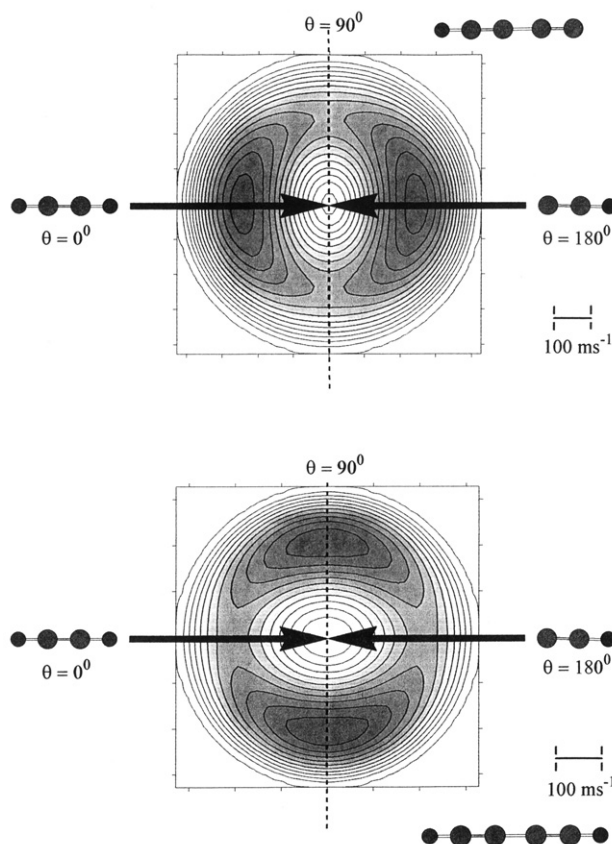
Fig. 3 Center-of-mass velocity flux contour maps for the $C_2D(X\ ^2\Sigma^+) + C_2H_2(X\ ^1\Sigma_g^+)$ reaction. Top: DCCCC + H$_2$ channel; bottom: DCCCCH + H channel. The contour lines connect points of constant intensities; light gray: minimum intensity; dark: maximum intensity; the direction of the C_2D beam is defined as 0° and of the acetylene beam as 180°.

velocity part of the contour plot. The atomic hydrogen loss was found to have a distribution maximum around 30–45 kJ mol^{-1}. This indicates that the exit transition state is rather tight. Channel 2 peaks at 3–5 kJ mol^{-1}, very close to zero translational energy, suggesting that the molecular hydrogen loss proceeds *via* a loose, product-like transition state. Finally the average energy released into the translational degrees of freedom was found to be 50–60 kJ mol^{-1} (channel 1) and 15–20 kJ mol^{-1} (channel 2).

The angular part of the flux contour plot supplies important information on the reaction dynamics involved. Here, both $I(\theta,u)$'s are forward–backward symmetric, suggesting that the reaction to form d1-diacetylene and d1-butadiynyl follows indirect scattering dynamics *via* bound C_4H_2D intermediate(s) which decompose(s) to DCCCCH + H (channel 1) and DCCCC + H$_2$ (channel 2). This symmetry documents further that the lifetimes of the fragmenting complex(es) are longer than the rotational period(s). However, the detailed shape of both $I(\theta,u)$ differs strongly. Whereas the flux contour map of channel 2 peaks at 90° with $I(90°)/I(0°) = 1.5$–1.4 ('sideways scattering'), channel 1 shows pronounced maxima at the poles (0° and 180°) and a minimum at $\theta = 90°$ ($I(180°)/I(90°) = 1.6$–1.5). The distinct shapes of the angular parts of both contour plots are dictated by the disposal of the total angular momentum J and are the result of geometrical constraints of the direction of the H/H$_2$ emission in the fragmenting C_4H_2D intermediate(s), *cf.* Section V.B. Based on these data and the fitting program,[18] the C_4HD/H pathways accounts for about 98–99%, whereas the C_4D/H_2 channel presents only a minor (1–2%) contribution at a collision energy of 26.1 kJ mol^{-1}.
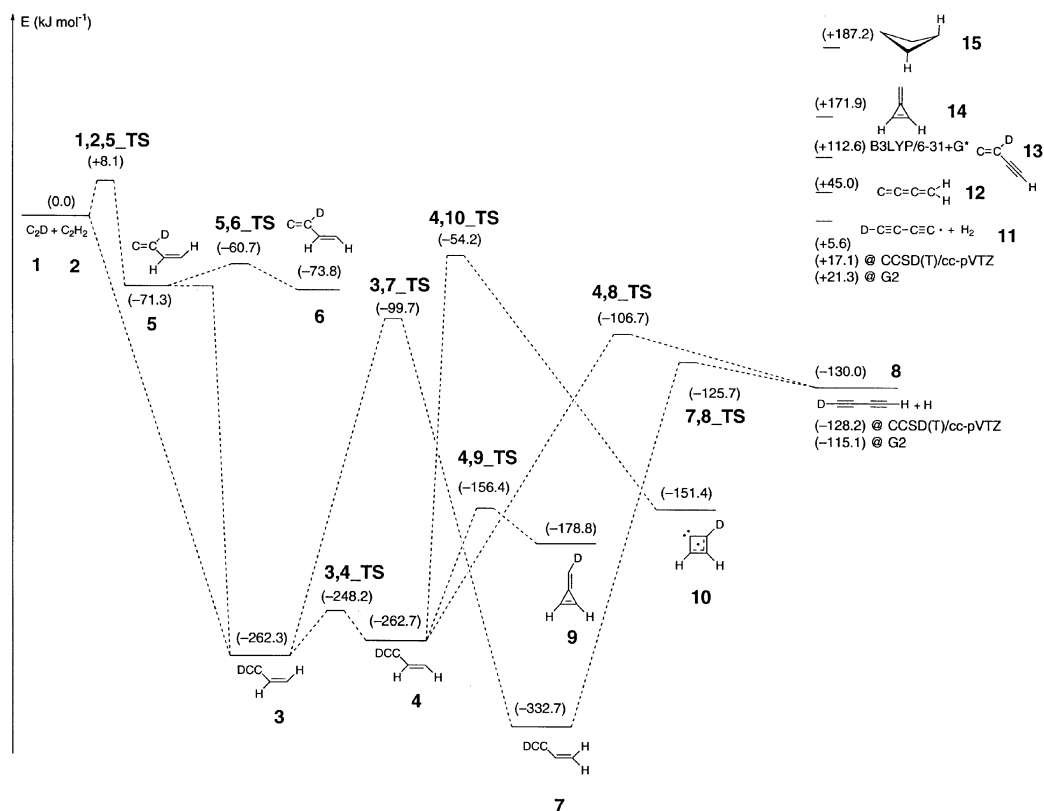
Fig. 4 Schematic representation of the C_4H_2D potential energy surface (UB3LYP/6-311+G** + ZPVE). Computational details are given in the text.

C. The *ab initio* doublet C_4H_2D potential energy surface (PES)

The computations reveal two possible entry channels for the reaction of the ethinyl radical (**1**) with acetylene (**2**). An attack of the terminal carbon atom of **1**, which holds the radical center, to the π-electron density of **2** proceeds without barrier and yields the *trans*-1-d-ethinylvinyl-2 radical (**3**) in a highly exothermic reaction (-262.3 kJ mol^{-1}, Figs. 4 and 5). A *cis–trans* isomerization from **3** to **4** progresses *via* a low barrier (**3,4_TS**) of only 14.1 kJ mol^{-1} (Figs. 4–6); hence, an ultrafast rearrangement with a near equal distribution of **3** and **4** is anticipated. The alternate entrance channel, in which the ethinyl radical (**1**) attacks acetylene (**2**) with the central carbon (**1,2,5_TS**), involves a barrier of 8.1 kJ mol^{-1} at UB3LYP/6-311+G**. Ceursters *et al.* have reported a similar value for this barrier (8.5 kJ mol^{-1} at UB3LYP/6-311++G**).[23] These authors further suggested that the height of the barrier is significantly increased (32 kJ mol^{-1}) when evaluated by CCSD(T)/6-311++G** single point energy computations. We have shown previously[24] that coupled cluster single point energies for related systems are highly dependent on the size of the basis set and, indeed, a single point energy computation with a larger basis set for **1,2,5_TS** at CCSD(T)/cc-pVTZ reproduces the DFT energy satisfyingly (8.6 kJ mol^{-1}). The initial intermediate for this reaction channel is the carbene-radical species **5**. Note that the two hydrogen atoms of the acetylene moiety are oriented *trans* to each other. This result is in disagreement with Ceurters *et al.* as they connected the *cis* isomer with the reactants **1** and **2**. It is not surprising that the resulting species **5** is highly unstable with respect to a 1,2-deuterium shift that yields **3**. Ceursters *et al.*[23] were unable to optimize the transition state for this process at the B3LYP/6-311++G** level and concluded on the basis of coupled cluster single point computations on a UHF optimized geometry
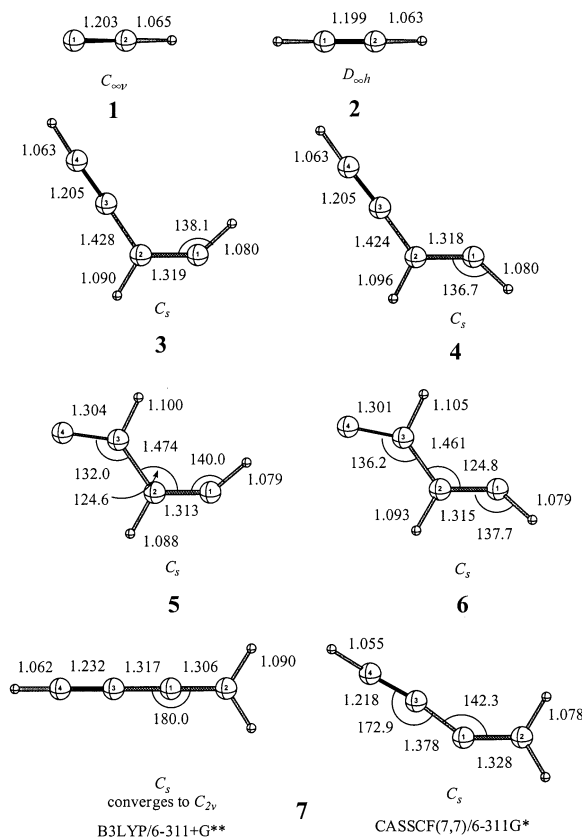
Fig. 5 Optimized geometries (UB3LYP/6-311+G**) of reactants, intermediates, and potential products on the C_4H_2D potential energy surface. Bond distances in Å and bond angles in degrees.
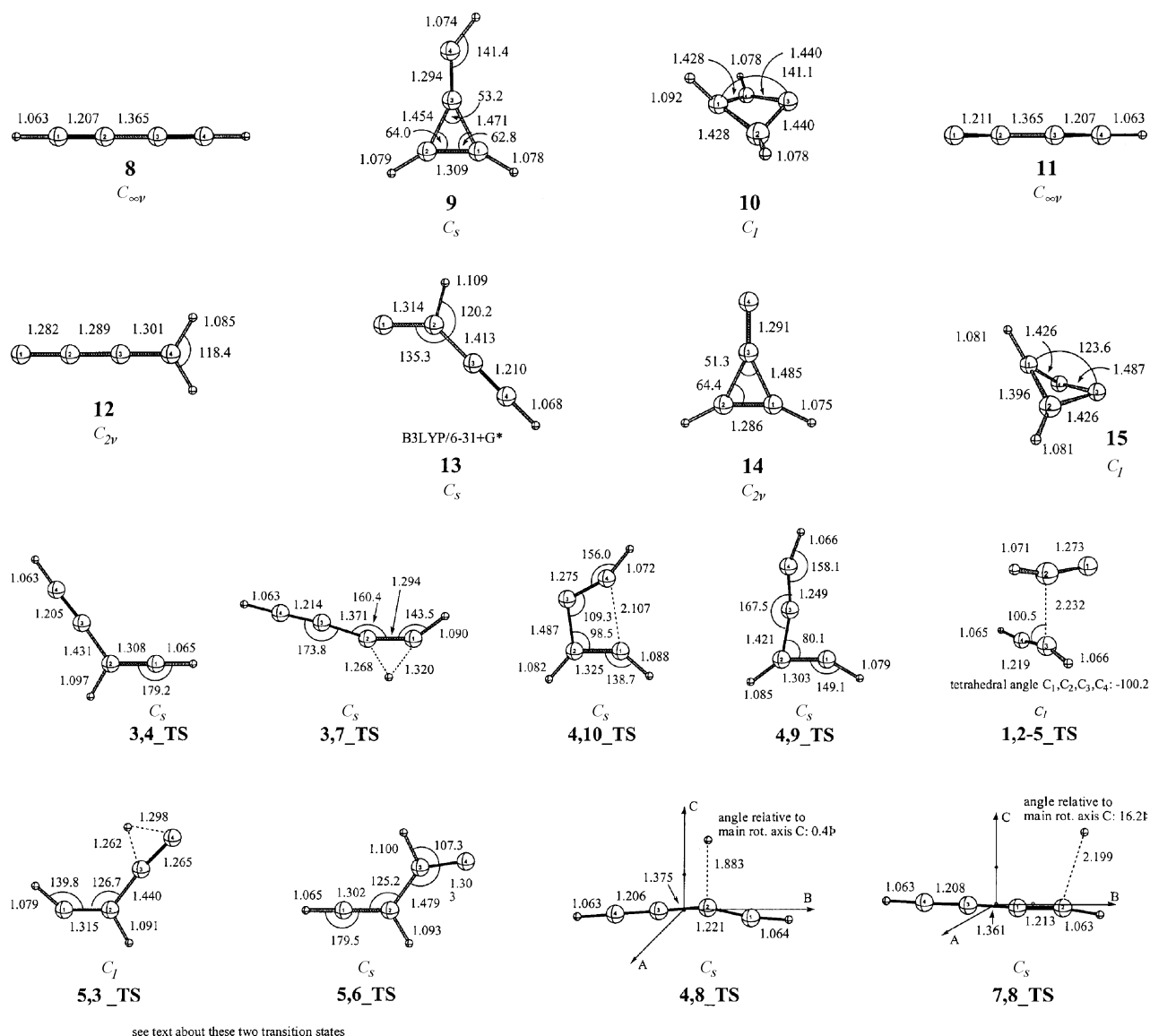
Fig. 6 Optimized geometries (UB3LYP/6-311+G**) of transition states on the C_4H_2D potential energy surface. Bond distances in Å and bond angles in degrees. The main rotational axes are indicated for relevant exit transition states to the products.

that the transition state **3,5_TS** lies only a few kJ mol^{-1} above **5**. We succeeded in optimizing this transition state at B3LYP/6-311+G**. Without considering the zero-point vibrational energy (ZPVE) correction, this structure is 3.5 kJ mol^{-1} higher in energy than **5**. Inclusion of ZPVE, however, leads to an energy below that of **5**. Hence, the transition state and the minimum **5** itself are artifacts of computing static points on a potential energy surface. A shallow minimum such as **5** might no longer exist under consideration of the zero-point vibrational energy (ZPVE). Therefore, attack of the ethynyl radical (**1**) to acetylene (**2**) *via* transition state **1,2,5_TS** yields intermediate **3** instantly. A *cis–trans* isomerization of the terminal hydrogen in **5** to yield **6** *via* **5,6_TS** is not a relevant reaction path, but is only included for completeness.

Besides *cis–trans* isomerization to **4**, **3** can undergo a [1,2]-hydrogen shift (**3,7_TS**) *via* a relatively high barrier of 162.6 kJ mol^{-1} to the global minimum of the C_4H_2D PES, the 1-d-ethinylvinyl-1 radical (**7**). The B3LYP/6-311+G** optimized geometry of **7** shows a linear arrangement of the carbon atoms (though optimized in C_s) and the lowest harmonic vibrational frequency, 86 cm^{-1} (A′), corresponds to the bending of the ethynyl substituent. At CASSCF(11,12)/6-311G* the structure is bent with a bonding angle of 142.3° of the C_2D substituent to the vinyl moiety. Therefore, all intermediates

3, 4, and **7** are C_s-symmetric doublet radicals with A′ ground states. Both **3** ensuing intermediates, **4** and **7**, can decompose to d1-diacetylene (**8**) under hydrogen atom emission *via* exit transition states **4,8_TS** and **7,8_TS**. The overall reaction exothermicity to form this product is computed to be -130 kJ mol^{-1} at UB3LYP/6-311+G**. This is matched satisfyingly by G2 (-115.1 kJ mol^{-1}) and CCSD(T)/cc-pVTZ single point energy (-128.2 kJ mol^{-1}) computations.

As verified experimentally (*cf.* Section V.), the d1-butadiynyl (DCCCC, (**11**)) radical presents a second reaction product which is formed *via* molecular hydrogen elimination. Therefore we investigated this pathway computationally as well. The calculated endothermicity for this product are 5.6 kJ mol^{-1} at UB3LYP/6-311+G**, 17.1 kJ mol^{-1} at CCSD(T)/cc-pVTZ//UB3LYP/6-311+G**, and 21.3 kJ mol^{-1} at G2. The comprehensible precursor for this process is intermediate **7** for which we optimized the geometry also at CASSCF(7,7)/6-311G*. All attempts to locate a transition state for an H_2-loss using DFT or CASSCF computations to form DCCCC (X $^2\Sigma^+$) failed. In the B3LYP optimized geometry of **7** the d-ethinyl moiety is almost collinear with the ethenyl moiety and the lowest harmonic vibrational frequency, 86 cm^{-1}, corresponds to the bending of the ethinyl substituent. It is important to note that butadiynyl marks the turning point within the series of C_nH radicals

($n = 2, 4, 6$) from a $^2\Sigma$ ground state in C_2H to a $^2\Pi$ ground state in C_6H.[25] The ground state of **11** is $^2\Sigma^+$, but the first excited state $^2\Pi$ is virtually isoenergetic.[26] This special feature might be the reason for this unexpected reaction channel and two potential energy surfaces that conically intersect or avoid crossing might be involved. We were, however, unable to locate such an intersection and a different explanation appears more attractive. Due to the computed low bending frequency, **7** might emit molecular hydrogen in a least-motion process without an exit-barrier in a (near-) linear conformation analogous to the DFT optimized structure. Further investigations are clearly necessary to resolve this molecular hydrogen elimination pathway.

Finally, we investigated all cyclic intermediates and alternative reaction products, which are higher in energy than **8**. Alternate pathways from **4** include cyclization reactions to **9** and **10** through high lying transition states **4,9_TS** and **4,10_TS**. The overall reaction energies of hypothetical deuterium atom losses to form products **14** and **15** are highly endothermic by 171.9 and 187.2 kJ mol^{-1}, respectively, and, hence, these paths are closed considering our experimental collision energy of 26.1 kJ mol^{-1}. Therefore, **9** and **10**, if formed at all can only react back to **4**. Note that the reaction sequence $4 \rightarrow 9 \rightarrow 4$ presents formally a migration of the ethinyl group from the C1 atom of acetylene to the C2 atom. Comparing the energies of **4,10_TS** with **4,9_TS** suggests that **10** should not be formed. An alternate product, the C_{2v} $^1A_1$ butatrienylidene **12** is 175.0 kJ mol^{-1} less stable than diacetylene and is therefore located above the energy of the separated reactants. The reaction energy to give **12** was calculated to be +45.0 kJ mol^{-1}. A carbene-type isomer, ethinylvinylidene (C_s, $^1A_1$, **13**) exists as well. This structure can only be formed in a highly endothermic reaction (+112.6 kJ mol^{-1}).

V. Discussion

A. Energetic considerations

In this section we compare experimentally obtained reaction energies of the molecular and atomic hydrogen elimination pathways with data derived from our electronic structure calculations to assign the reaction products. The situation of channel 1, *i.e.* the assignment of the C_2D *versus* H exchange pathway to form a C_4HD isomer, is straightforward, because **8** and **13** are the only feasible C_4HD isomer products. The electronic structure calculations predict reaction energies of -130.0 kJ mol^{-1} and $+112.6$ kJ mol^{-1} for diacetylene (**8**) and singlet ethinylvinylidene (**13**), respectively. Therefore, with only a collision energy of 26.1 kJ mol^{-1} at disposal, formation of **13** can be excluded. However, the experimentally derived reaction energy to form d1-diacetylene of -110 to -120 kJ mol^{-1} correlates very nicely with our theoretical data.

Channel 2 was fit with a $C_4D + H_2$ pathway. Based on our computations, the reaction to form butadiynyl DCCCC (X $^2\Sigma^+$) **11** plus molecular hydrogen was found to be slightly endothermic by 5.6 kJ mol^{-1}, whereas our experiments depict reaction energies between $+4$ kJ mol^{-1} and -6 kJ mol^{-1}. The first electronically excited state ($^2\Pi$) of butadiynyl is only 2.9–3.4 kJ mol^{-1} higher in energy[27] and could account for this channel as well within our error limits. We would like to recall that in principle a molecule with the gross formula C_4H_2 also could contribute to $m/z = 50$. The electronic structure calculations, however, demonstrate explicitly that the C_4H_2 isomers **12, 14,** and **15** are endothermic by $+45.0$ kJ mol^{-1}, $+171.9$ kJ mol^{-1}, and $+187.2$ kJ mol^{-1}, respectively. Since the collision energy in our experiments was only 26.1 kJ mol^{-1}, these products cannot be formed under our experimental conditions. Therefore we conclude, that the butadiynyl radical (**11**) in its $^2\Sigma^+$ and/or $^2\Pi$ state is formed. To summarize, our high-energy

cutoffs establish two reaction products, d1-diacetylene (**8**) and the butadiynyl radical (**11**).

B. Center-of-mass angular distribution considerations and exit transition states

The detailed shape of the angular part of the center-of-mass flux contour map is directed by the disposal of the total angular momentum J. In our crossed beam experiment, each reactant undergoes a supersonic expansion and rotational cooling occurs. Hence the total angular momentum is present initial as orbital angular momentum L. The polyatomic products of channel 1 and 2 can be rotationally excited giving rise to a rotational angular momentum j'. Denoting the final orbital angular momentum as L', angular momentum conservation dictates $J \approx L \approx L' + j'$. The final recoil velocity vector, v', is in a plane perpendicular to L' and therefore, when the rotational excitation of products is significant, v' is not in a plane perpendicular to J. When j' is not zero, the probability distribution for the scattering angle θ, which is the center-of-mass angle between the initial relative velocity v and v', depends on the values of J, M and M' where M and M' are the projections of J on the initial and final relative velocity, respectively. For instance, if the complex dissociates preferentially with low M' values, the final velocity v' is almost perpendicular to J and therefore v' and v are almost parallel; in this case, the product intensity will be mainly confined to the poles, $\theta = 0°$ and $\theta = 180°$, similar to the case of no product rotational excitation. On the contrary, when the collision complex dissociates mainly with high M' values, the final relative velocity will be almost parallel to J and perpendicular to v, and the products will be preferentially scattered at $\theta = 90°$.

In the case of channel 1 (H atom loss), the angular part of the flux contour peaks at $\theta = 90°$ ('sideways scattering'). This finding documents that the most probable direction of the H atom release is parallel to J as found previously in the systems $F + C_6D_6 \rightarrow C_6D_5F + D$,[28] $CN + C_6D_6 \rightarrow C_6D_5CN + D$,[29] $CN + C_2H_2 \rightarrow HCCCN + H$,[30] and $C_2D + CH_3CCH \rightarrow CD_3CCCCD + H$.[31] On the other hand, the molecular hydrogen (channel 2) is released predominantly perpendicular to the total angular momentum vector and, hence, in the plane of the fragmenting C_4H_2D complex. Therefore, the theoretically investigated exit transition state(s) from the decomposing complex(es) to the products must account for this experimental finding.

Figure 6 shows the computed structures of two exit transition states of the H atom loss pathway connecting the intermediates **4** and **7** with the DCCCCH + H products. Based on these considerations, **4,8_TS** can account for the experimentally found sideways peaking of the flux contour plot. Here, the electronic structure calculations predict an angle between the C axis (which in turn is parallel to J) and the direction of the leaving hydrogen atom of 0.4°; this matches the predicted value of 0° which arises from a H loss strictly parallel to J, perfectly. Therefore, we can conclude that the H atom is emitted parallel to J and almost perpendicular to the plane defined by the four heavy carbon atoms documenting that $3 \rightarrow 4 \rightarrow 8 + H$ should be the dominant reaction pathway compared to $3 \rightarrow 7 \rightarrow 8 + H$. Further evidence for this conclusion is provided by the distribution maximum of the relative velocity part of the contour plot (*cf.* section IV. B) that suggests an exit transition state for this process locate 30–45 kJ mol^{-1} above the product (**8**). This order of magnitude is in reasonable agreement with the computed value of 23.3 kJ mol^{-1} for **4,8_TS**. The alternate exit transition state **7,8_TS** lies only 4.3 kJ mol^{-1} above the product **8**. Furthermore, it does not emit the hydrogen atom parallel to J but rather at an angle of 16.2°.

C. The actual reaction pathway

The identification of two reaction products (d1-diacetylene and d1-butadiynyl), the assignment of indirect reactive scattering dynamics, the calculated geometry of the exit transition state(s), and the calculated potential energy surface untangle finally the underlying reaction dynamics of the C_2D (X $^2\Sigma^+$) $+ C_2H_2$ (X $^1\Sigma_g^+$) reaction. The d1-ethinyl radical adds to the π electron density of the carbon–carbon triple bond of the acetylene molecule without entrance barrier. This forms a *trans* 1-d-ethinylvinyl-2 collision complex **3** which isomerizes rapidly to its *cis* form **4** on the $^2A'$ surface; both structures are stabilized by 262 kJ mol^{-1} and 265 kJ mol^{-1} with respect to the separated reactants. Since the barrier of a *cis–trans* conversion ranges well below the total available energy, we can expect an ultrafast isomerization process as well as an equal concentration of **3** *versus* **4**. Both 1-ethinylvinyl-2 radicals resemble prolate asymmetric top molecules, and the heavy atoms are expected to rotate nearly in a molecular plane perpendicular to the total angular momentum vector ***J***. In planetary atmospheres and in molecular clouds, where average translational temperatures are between 10 and 100 K, an alternative entrance channel *via* **1,2,5_TS** *via* an entrance barrier of 8.1 kJ mol^{-1} is certainly closed.

The intermediates **3** and **4** were found to undergo three distinct reaction channels. First, **4** decomposes *via* a hydrogen atom emission to form d1-diacetylene (DCCCCH(X $^1\Sigma^+$)) *via* a tight exit transition state located 23.7 kJ mol^{-1} above the products (channel 1). The latter is confirmed experimentally since the flux contour map shows a distribution maximum which corresponds to 30–40 kJ mol^{-1}. Therefore, the reverse reaction, *i.e.* addition of a hydrogen atom to the carbon–carbon triple bond of the d1-diacetylene molecule involves a significant entrance barrier (*cf.* section V.D). As verified experimentally ('sideways scattering') and by our electronic structure calculations, the H atom loss proceeds almost parallel to the total angular momentum vector ***J*** and, hence, perpendicular to the molecular plane of the decomposing complex **4**. This leaves the d1-diacetylene molecule highly rotationally excited (B-like rotations). The calculated well depth of 265 kJ mol^{-1} of **3** and **4** can account for the observed forward–backward symmetric contour plot.

To a minor amount, **3** undergoes a [1,2]-hydrogen shift to the thermodynamically more stable 1-d-ethinylvinyl-1 radical **7**. The latter is the global minimum of the C_4H_2D potential energy surface and is stabilized by 332.7 kJ mol^{-1} with respect to the reactants. The lowest bending frequencies of only 86 and 232 cm^{-1} verify the extreme floppiness of this structure. Intermediate **7** fragments *via* molecular hydrogen loss to the butadiynyl radical *via* molecular hydrogen loss (channel 2); this H_2 elimination occurs in the molecular plane of the decomposing complex. Similar to channel 1, the decomposing complex resides in a deep potential energy well; this is well reflected in the forward–backward symmetric contour plot of channel 2. The experiments suggest a loose exit transition state with a very low, probably no, exit barrier. Since the long-lived complex **7** fragments to DCCCC $+ H_2$, we have to concede that the thermodynamically more favorable pathway *via* an atomic hydrogen elimination from **7** to DCCCCH $+$ H should be open as well (channel 3). However, based on the shape of contour plots and the experimentally found sideways peaking, this pathway is expected to be less prominent compared to channel 1. Finally, we would like to stress that no other isomers were formed. However, although the three-membered ring structure **9** plays no role in the active chemistry, the existence of this intermediate might increase the lifetime of the decomposing complex **4** and could favor an energy randomization.

D. Comparison with the reverse reaction of $C_4H_2 + H$

It is interesting to compare the reaction mechanism in the C_2D/C_2H_2 system we have elucidated with the reaction of atomic hydrogen plus diacetylene. The calculations and, to some extent, the release of translational energy to the C_4HD plus H products leads to the inference of an exit channel barrier (**4,8_TS**) of 23 kJ mol^{-1}. Kinetic studies of the reversed reaction suggest activation energy for addition of atomic hydrogen to C_4H_2 between 4.2 kJ mol^{-1}[32] and 9.8 kJ mol^{-1}.[33] At first glance, these data seem to contradict each other. However, a closer look at the pertinent potential energy surface (Fig. 4) resolves this issue. Here, the hydrogen atom reacts with the diacetylene molecule preferentially *via* transition state **7,8_TS** to **7** rather through **4,8_TS** to form **4**, since the barrier of the latter transition state is 19.0 kJ mol^{-1} higher than **7,8_TS**. The computed entrance barrier of only 4.3 kJ mol^{-1} shows a similar order of magnitude as the activation barrier determined from kinetic studies. This suggests that the addition of a hydrogen atom to diacetylene may indeed occur *via* transition state **7,8_TS**.

E. Comparison with the reaction of CN(X $^2\Sigma^+$) $+ C_2H_2$

Reactions of the linear C_2D and the CN radicals exhibit striking similarities, but also significant differences. Firstly, the two species are isoelectronic with $^2\Sigma^+$ ground states. Initial attack of the C_2D/CN radical on acetylene forms C_s symmetric *cis/trans* C_2H_2X (X $= C_2D$, CN) complexes on the $^2A'$ surface which are stabilized by 240–270 kJ mol^{-1} which account for the indirect scattering dynamics found in both systems. Secondly, the collision complexes can undergo [1,2]-H migration to form thermodynamically more stable $XCCH_2$ radicals, which are bound by 290–330 kJ mol^{-1}. Thirdly, an H atom elimination pathway from C_2H_2X *via* a tight (22–24 kJ mol^{-1} above the reaction product) exit transition state dominates the reaction. In both cases, the H atom is emitted almost parallel to the total angular momentum vector and, hence, perpendicular to the plane of the decomposing complex. The competing atomic hydrogen elimination from C_2H_2X *via* a loose, product-like (4–7 kJ mol^{-1}) exit transition state is found to be a less important channel. Finally, the exothermicities of the formation of the main reaction products are comparable (90–120 kJ mol^{-1}).

Whereas the CN/C_2H_2 system goes through an osculating complex at a collision energy of 27.0 kJ mol^{-1}, the reaction of C_2D with C_2H_2 involves long-lived complexes. Two effects are responsible for this difference. Firstly, the additional atom of the C_2D *versus* the CN reactant increases the number of vibration modes by three. Secondly, the low frequency wagging/bending modes of the C–D group might increase the lifetime even further. This is well reflected in an enhanced fraction of energy channeling into the translational motion. Finally, we were not able to detect a molecular hydrogen loss pathway in the CN/C_2H_2 reaction. This pathway is endothermic by about 35 kJ mol^{-1} in the CN/C_2H_2 system and, hence, could not occur at a maximum collision energy of 27.0 kJ mol^{-1}.[34]

Most important, the elucidated reaction dynamics can confirm recent kinetic investigations of the ethinyl and cyano radical reactions with acetylene. Employing the CRESU (Cinetique de Reaction en Ecoulement Supersonique Uniforme) apparatus in Birmingham, rate constants of $2.27 \pm 0.29 \times 10^{-10}$ cm^3 s^{-1} ($T = 15$ K) and $4.60 \pm 0.25 \times 10^{-10}$ cm^3 s^{-1} ($T = 25$ K) have been measured at similarly low temperatures for the C_2H/C_2H_2[7] and CN/C_2H_2 reactions, respectively.[35] As the authors pointed out, the rate constants of the ethinyl radical reactions are systematically lower by a factor of two compared to the cyano radical systems. Crossed beam studies combined with electronic structure calculations demonstrated that the cyano radical can add to the unsaturated bond with the carbon and nitrogen atom, thus forming a cyano- or isocyano intermediate,[36] *cf.* Fig. 7. Since the formation of isonitriles is forbidden energetically, those isocyano intermediates were found to rearrange to the corresponding
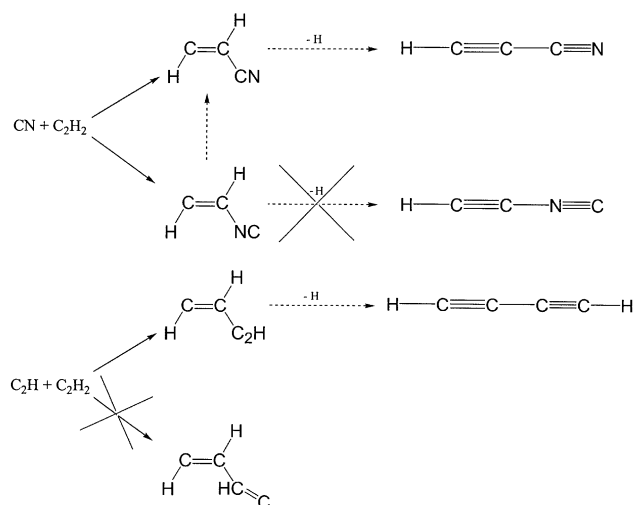
Fig. 7 Schematic presentation of the most important reaction pathways in the reactions of cyano and ethinyl radicals with acetylene; pathways which are closed are crossed out.

cyano intermediates *via* a three-membered ring transition state to the nitrile isomer which in turn loses an H atom. However, the ethinyl radical can add to the π-bond without barrier only with the terminal carbon atom, addition of the HC-group involves transition state **1,2,5_TS** and, hence, a barrier of 8.1 kJ mol^{-1} which cannot be overcome in the low temperature CRESU experiments. Therefore, a simple explanation for the observed lower rate constants of the C_2H compared to the CN reaction might be that only half of the collisions of the ethinyl radical are reactive.

VI. Conclusions

The chemical reaction dynamics of the reaction of d1-ethinyl C_2D (X $^2\Sigma^+$), with acetylene, C_2H_2 (X $^1\Sigma_g^+$), are investigated in a crossed beam experiment forming d1-diacetylene, DCCCCH (X $^1\Sigma^+$), and the d1-butadiynyl radical, DCCCC following atomic and molecular hydrogen emission, respectively. Three reaction channels were observed. Our data reveal that the reaction has no entrance barrier, follows indirect scattering dynamics *via* complex formation, and is initiated by an attack of the C_2D (X $^2\Sigma^+$) radical to the carbon–carbon triple bond of the acetylene molecule. This forms a C_s symmetric $^2A'$ *trans*-1-d-ethinylvinyl-2 (HCCHC$_2$D, **3**) collision complex which rearranges rapidly to the *cis* form **4**. The four heavy atoms are rotating in a plane almost perpendicular to the total angular momentum vector J around the C axis of the complex. The *cis*-HCCHC$_2$D intermediate **3** fragments predominantly *via* H atom emission through a tight exit transition state located 23 kJ mol^{-1} above the d1-diacetylene, HCCCCD (X $^1\Sigma^+$) and H($^2S_{1/2}$) products (channel 1). To a minor extent, the 1-d-ethinylvinyl-1 radical (**7**), which was formed upon a [1,2]-H shift of the initial intermediate **3**, was found to emit molecular hydrogen forming the d1-butadiynyl radical (DCCCC) (channel 2). Channel 3 results from an H atom loss of H$_2$CCCCD (**7**) *via* a loose exit transition state located only 4 kJ mol^{-1} above the products. Further studies of this reaction should focus on the exact reaction energy of the molecular hydrogen loss pathway. Likewise, the location of the exit transition state, if one exists, and the role of an excited surface remain to be solved.

The explicit identification of two reaction products, diacetylene (**8**) and the butadiynyl radical (**11**), demonstrate that the neutral–neutral reaction of ethinyl radicals with acetylene represents an efficient pathway to produce diacetylene molecules in planetary atmospheres in those regions where density

profiles of photolytically generated ethinyl radicals and acetylene molecules overlap. In contradiction to earlier assumptions, our investigations suggest the formation of a second product, the butadiynyl radical. Previously, this pathway has not been considered in photochemical models of hydrocarbon rich atmospheres since the synthetic route to butadiynyl was postulated to proceed solely *via* photodissociation of diacetylene. The reaction to form butadiynyl could be slightly endothermic. If so, only the species in the long tail of the Maxwell–Boltzmann distribution could react to give butadiynyl in planetary atmospheres. Alternatively, photodissociation of acetylene yields vibrationally excited ethinyl radicals.[37] This vibrational excitation can be incorporated into the reaction coordinate to form butadiynyl. However, if the reaction to form the butadiynyl turns out to be slightly endothermic, it is inhibited in cold molecular clouds as translational temperatures of only 10 K prevail. Nevertheless, our finding might have significant implications for the understanding and quantification of the atmospheric diacetylene balance in hydrocarbon rich planetary atmospheres. Once implemented into atmospheric models, this second pathway will reduce the diacetylene production rate of the C_2H/C_2H_2 system. Further, butadiynyl can react with diacetylene to yield tetraacetylene (C_8H_2) thus offering an additional diacetylene sink. Both effects together can refine recent models of Titan's atmosphere which predict a fivefold larger amount of diacetylene than that actually observed by Voyager. Future chemical models must take this one-step synthetic route to C_4H into account as an important alternative to multiple reaction sequences *via* C_4H_2. Last but not least, we identified four radical intermediates **3, 4, 7,** and **9**. Under our single collision conditions, these species are formed with extremely high internal excitation, and their lifetimes are of the order of a few picoseconds. Hence, they fragment before reaching the detector. However, in the denser atmospheres of Titan and Saturn, ternary collisions may have a significant impact on the chemistry and can divert the internal energy. This will stabilize those intermediates. Most importantly, these radicals can undergo subsequent reactions with C_2H_2, C_2H, or C_4H_2 to form even more complex molecules such as C_6H_5, C_6H_4, C_6H_5, C_8H_5, and C_8H_4 isomers, extremely unstable species which have been only partly included into chemical reaction networks of these solar system environments.

References

1 M. Kolbuszewski, *Astrophys. J.*, 1994, **432**, L63.
2 R. E. Brady, C. Lakshminarayan, R. K. Frost and T. S. Zwier, *Science*, 1992, **258**, 1630.
3 R. K. Frost, *J. Am. Chem. Soc.*, 1998, **118**, 4451.
4 Y. L. Yung, M. Allen and J. P. Pinto, *Astrophys. J. Suppl*, 1984, **55**, 465.
5 N. S. Smith, Y. Benilan and P. Bruston, *Planet. Space Sci.*, 1998, **46**, 1215 (Larger mixing ratios of diacetylene and other molecules are predicted in these models than actually observed.).
6 Huygens – Science, Payload, and Mission, ESA Special Publication 1177, ESA, Noordwijk, 1997.
7 D. Chastaing, P. L. James, I. R. Sims and I. W. M. Smith, *Faraday Discuss.*, 1998, **109**, 165.

8   Using C_2D compared to C_2H has the advantage to identify if the hydrogen atom is lost from the acetylene (H loss) or from the ethynyl radical (D loss).

9   Mixing ratios of acetylene were determined between 2×10^{-6} and 1×10^{-8} on Jupiter, Saturn, Uranus, Neptune, and Titan L (*a*) F. Raulin and C. Frere, *J. Br. Interplanetary Soc.*, 1989, **42**, 411; (*b*) G. R. Gladstone, M. Allen and Y. L. Yung, *Icarus*, 1996, **119**, 52.

10 M. C. Gazeau, H. Cottin, V. Vuitton, N. Smith and F. Raulin, *Planetary Space Sci.*, 2000, **48**, 437.

11 N. Balucani, O. Asvany, L. C. L. Huang, Y. T. Lee, R. I. Kaiser and Y. Osamura, *Planetary Space Sci.*, 2000, **48**, 447.

12 R. I. Kaiser and A. G. Suits, *Rev. Sci. Instrum.*, 1995, **66**, 5405.

13 R. I. Kaiser, J. W. Ting, L. C. L. Huang, N. Balucani, O. Asvany, Y. T. Lee, H. Chan, D. Stranges and D. Gee, *Rev. Sci. Instrum.*, 1999, **70**, 4185.

14 R. I. Kaiser, C. C. Chiong, O. Asvany, Y. T. Lee, F. Stahl, P. v. R. Schleyer and H. F. Schaefer, *J. Chem. Phys.*, 2001, **114**, 3488.

15 R. I. Kaiser, C. Ochsenfeld, M. Head-Gordon, Y. T. Lee and A. G. Suits, *Science*, 1996, **274**, 1508.

16 R. I. Kaiser, A. M. Mebel, N. Balucani, Y. T. Lee, F. Stahl, P. v. R. Schleyer and H. F. Schaefer, *Faraday Discuss.*, 2001, **119**, 51.

17 (*a*) G. O. Brink, *Rev. Sci. Instrum.*, 1966, **37**, 857; (*b*) N. R. Daly, *Rev. Sci. Instrum.*, 1966, **31**, 264.

18 M. S. Weis, Ph.D. Thesis, University of California, Berkeley, 1986.

19 M. J. Frisch, G. W. Trucks, H. B. Schlegel, G. E. Scuseria, M. A. Robb, J. R. Cheeseman, V. G. Zakrzewski, J. A. Montgomery, Jr., R. E. Stratmann, J. C. Burant, S. Dapprich, J. M. Millan, A. D. Daniels, K. N. Kudin, M. C. Strain, O. Farkas, J. Tomasi, V. Barone, M. Cossi, R. Cammi, B. Mennucci, C. Pomelli, C. Adamo, S. Clifford, J. Ochterski, G. A. Petersson, P. Y. Ayala, Q. Cui, K. Morokuma, D. K. Malick, A. D. Rabuck, K. Raghavachari, J. B. Foresman, J. Cioslowski, J. V. Ortiz, B. B. Stefanov, G. Liu, A. Liashenko, P. Piskorz, I. Komaroni, R. Gomperts, R. L. Martin, D. J. Fox, T. Keith, M. A. Al-Laham, C. Y. Peng, A. Nanayakkara, C. González, M. Challacombe, P. M. W. Gill, B. Johnson, W. Chen, E. S. Replogle, J. A. Pople, *Gaussian 98, Revision A.7*, Gaussian Inc., Pittsburgh, PA, 1999.

20 GAMESS: See H. Umeda, S. Koseki, U. Nagashima and M. W. Schmidt, *J. Comput. Chem.*, 2001, **22**, 1243 and references cited therein.

21 ACES II: Quantum Theory Project, University of Florida, J. F. Stanton, J. Gauss, J. D. Watts, M. Nooijen, N. Oliphant, S. A. Perera, P. G. Szalay, W. J. Lauderdale, S. A. Kucharski, S. R. Gwaltney, S. Beck, A. Balková, D. E. Bernholdt, K. K. Baeck, P. Rozyczko, H. Sekino, C. Hober and R. J. Bartlett. Integral packages included are VMOL (J. Almlöf and P. R. Taylor); VPROPS (P. Taylor) ABACUS; (T. Helgaker, H. J. Aa. Jensen, P. Jørgensen, J. Olsen, and P. R. Taylor).

22 L. A. Curtiss, K. Raghavachari, G. W. Trucks and J. A. Pople, *J. Chem. Phys.*, 1991, **94**, 7221.

23 B. Ceursters, H. M. T. Nguyen, J. Peeters and M. T. Nguyen, *Chem. Phys.*, 2000, **262**, 243.

24 F. Stahl, P. v. R. Schleyer, H. F. Bettinger, R. I. Kaiser, Y. T. Lee and H. F. Schaefer III, *J. Chem. Phys.*, 2001, **114**, 3476–3487.

25 D. E. Wohn, *Chem. Phys. Lett.*, 1995, **244**, 45.

26 (*a*) M. Kolbuszewski, *ApJ.*, 1994, **432**, L63; (*b*) A. L. Sobolewski and L. Adamowicz, *J. Chem. Phys.*, 1995, **102**, 394.

27 S. Graf, J. Geiss and S. Leutwyler, *J. Chem. Phys.*, 2001, **114**, 4542.

28 K. Sobatake, J. M. Parson, Y. T. Lee and S. A. Rice, *J. Chem. Phys.*, 1973, **59**, 1427.

29 N. Balucani, O. Asvany, A. H. H. Chang, S. H. Lin, Y. T. Lee, R. I. Kaiser, H. F. Bettinger, P. v. R. Schleyer and H. F. Schaefer III, *J. Chem. Phys.*, 1999, **111**, 7457.

30 L. C. L. Huang, A. H. H. Chang, O. Asvany, N. Balucani, S. H. Lin, Y. T. Lee, R. I. Kaiser and Y. Osamura, *J. Chem. Phys.*, 2000, **113**, 8656.

31 F. Stahl, P. v. R. Schleyer, R. I. Kaiser, Y. T. Lee and H. F. Schaefer III, *J. Chem. Phys.*, 2001, **114**, 3476.

32 J. Warnatz, in *Rate coefficients in the C/H/O system, Combustion Chemistry*, ed. W.C. Gardiner, Jr., Springer, New York, 1984, p. 197.

33 D. F. Nava, M. B. Mitchell and L. J. Stief, *J. Geophys. Res.*, 1991, **91**, 4585.

34 R. I. Kaiser and N. Balucani, *Acc. Chem. Res.*, 2001, **34**, 699.

35 I. R. Sims, J. L. Queffelec, A. Defrance, D. Travers, B. Rowe, L. Herbert, J. Karthauser and I. W. M. Smith, *Chem. Phys. Lett.*, 1993, **211**, 461.

36 L. C. L. Huang, A. H. H. Chang, O. Asvany, N. Balucani, S. H. Lin, Y. T. Lee, R. I. Kaiser and Y. Osamura, *J. Chem. Phys.*, 2000, **113**, 8656.

37 A. M. Wodtke and Y. T. Lee, *J. Chem. Phys.*, 1998, **89**, 4744.